DALTON
FULL PAPER

Novel coordination modes of partially hydrogenated diyne ligands on metal carbonyl clusters†

Lionel P. Clarke, John E. Davies, Paul R. Raithby *‡ and Gregory P. Shields

Department of Chemistry, Lensfield Road, Cambridge, UK CB2 1EW.
E-mail: p.r.raithby@bath.ac.uk

Received 21st August 2000, Accepted 17th October 2000
First published as an Advance Article on the web 28th November 2000

The reaction of $[Ru_4H_4(CO)_{12}]$ with the 1,3-diynes RC_2C_2R (R = Me, $SiMe_3$ or Ph) under reflux conditions, in heptane, yielded the tetraruthenium clusters $[Ru_4(CO)_{12}\{\mu_4\text{-}\eta^1:\eta^2:\eta^2:\eta^1\text{-}(RCH_2C_3R)\}]$ **1** and $[Ru_4(CO)_{12}\{\mu_4\text{-}\eta^2:\eta^1:\eta^1:\eta^2\text{-}[RC(H)C]_2\}]$ **2** (R = Me **a**, $SiMe_3$ **b** or Ph **c**) in good yield. In **1** a 1,1-dihydrogenation occurs to generate an allene-1,3-diyl ligand, which coordinates to the butterfly Ru_4 face in a novel $\eta^1:\eta^2:\eta^2:\eta^1$ mode, whereas in **2** a 1,4-dihydrogenation occurs to yield a 1,3-diene-2,3-diyl ligand bound to the Ru_4 butterfly *via* four C atoms in a $\eta^2:\eta^1:\eta^1:\eta^2$ mode. In addition, the trinuclear cluster $[Ru_3(\mu\text{-}H)(CO)_9\{\mu_3\text{-}\eta^2:\eta^2:\eta^1\text{-}[RCH_2C_2CHPh)]$ **3c** (R = Ph) is produced as a result of 1,1,4 trihydrogenation of the diyne and loss of one ruthenium vertex. The clusters have fully been characterised spectroscopically, and the crystal structures of **1a**,**1c 2a**,**2c** and **3c** determined.

The reactions of alkynes with ruthenium and osmium cluster carbonyls have been thoroughly investigated,[1] but less attention has been paid, until recently, to those of polyynes with clusters. These extended carbon chains have the potential to show a greater range of coordination modes than alkynes, and have been shown to link small cluster units together.[2] There also remains the appealing analogy between the nature of the interactions between unsaturated organic ligands on a cluster and those of organic molecules on a catalytic metal surface,[3] so that the study of cluster–polyyne interactions may provide useful information.

The reactions between diyne ligands and ruthenium and osmium clusters are of particular current interest. Several research groups have investigated the thermolysis reactions of $[Ru_3(CO)_{12}]$, $[Os_3(CO)_{12}]$ and $Ru_3(CO)_{10}(NCMe)_2]$ with a variety of functionalised diynes and identified a number of mono-, di-, tri- and tetra-nuclear cluster products.[4–6] These reactions involve metal–metal bond cleavage, C≡C bond activation, intramolecular cyclisation and ligand coupling. In partial contrast, when "stabilised" clusters such as $[Ru_3(CO)_{10}(dppm)]$ and $[Ru_4(CO)_{13}(\mu_3\text{-PPh})]$ undergo reactions with RC_2C_2R (R = Me, Ph or $SiMe_3$) the cluster nuclearity is maintained, but a variety of bonding modes of the diyne are observed.[7,8] The presence of the chelating or capping phosphorus donor ligands inhibits metal–metal bond cleavage. In several cases, similar or related products to those observed from cluster carbonyls and diynes are observed in reactions involving coupling of alkynes[9,10] or alkynes and $P(C_2R)_2$ ligands on clusters surfaces.[11] Recently, related ruthenium clusters that contain extended carbon–chain ligands have been obtained by coupling of alkynes with bare "C_2" units contained in preformed cluster precursors.[12]

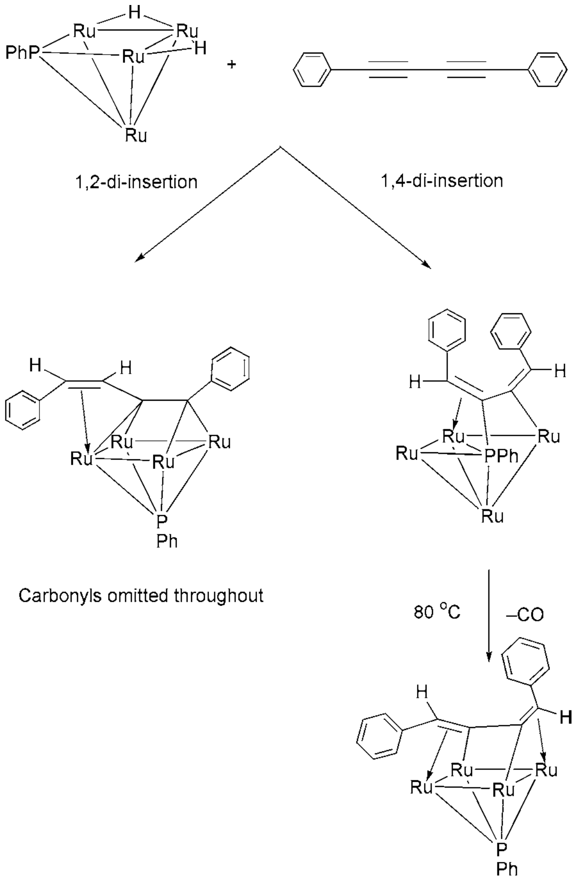

Scheme 1

Of particular relevance to the investigation reported here is the key point that reactions of diynes with hydrido clusters differ from those described above in that hydrogenation of the diyne may also occur. In one of the few reported examples the reaction of $[Ru_4(\mu\text{-}H)_2(CO)_{12}(\mu_3\text{-PPh})]$ with PhC_2C_2Ph, hydrogenation occurs at both the 1,2 positions to generate $[Ru_4(CO)_{11}(\mu_4\text{-PPh})\{\mu_4\text{-}\eta^1:\eta^1:\eta^1:\eta^3\text{-}PhC(H)C(H)C_2Ph\}]$ and at the 1,4 positions, yielding $[Ru_4(CO)_{12}\{\mu_4\text{-}\eta^1:\eta^1:\eta^1:\eta^3\text{-}P(Ph)C\text{-}[C(H)Ph]CC(H)Ph\}]$ (Scheme 1).[13] The latter transforms at 80 °C with loss of CO to a cluster based on a square of Ru atoms with a μ_4-PPh ligand and a $\mu_4\text{-}\eta^1:\eta^2:\eta^2:\eta^1$-1,3-diene-2,3-diyl ligand bound to the opposite square face. This

---

† Dedicated to the memory of Dr Ron Snaith who will be remembered for his outstanding contribution to inorganic chemistry, and for all the encouragement and friendship that he gave to all his students and colleagues.

‡ Current address: Department of Chemistry, University of Bath, Claverton Down, Bath, UK BA2 7AY.

DOI: 10.1039/b006810l

coordination mode, which could be viewed as two linked σ,π-vinyl ligands, is relatively uncommon, although it has also been observed in the structure of $[Ru_4(CO)_{12}(\mu_4\text{-}C_8H_{10})]$ obtained by the 2,3 dehydrogenation of octa-1,3-diene in the reaction with $[Ru_3(CO)_{12}]$.[14] In addition to the hydrogenation of diynes and dehydrogenation of dienes, dienediyl ligands may be obtained by an alkyne coupling reaction on a metal cluster.[1] These typically afford 1,3-diene-1,4-diyl ligands but, where $SiMe_3$ substituents are present on the alkynes, a 1,2-dilyl shift may occur to generate a coordinated 1,3-diene-1,3-diyl moiety.[15] Similarly, where one alkyne possesses a terminal H atom, alkyne coupling may be associated with a 1,3 hydrogen shift (*via* the metal cluster) to produce a 1,3-diene-1,2-diyl-(3-en-1-yne) ligand, which coordinates typically in a $\mu_3\text{-}\eta^1:\eta^2:\eta^3$ manner to a trinuclear cluster.[16]

Here, we report the results of an investigation into the reaction of the hydrido cluster $[Ru_4H_4(CO)_{12}]$ with the diynes RC_2C_2R (R = Me, $SiMe_3$ or Ph). The results are summarised in Scheme 2. The objective was to determine the positions of hydrogenation, in the absence of phosphorus-containing ligands on the cluster, and to explore the possibility of transferring more than two hydrogen atoms to the diyne.

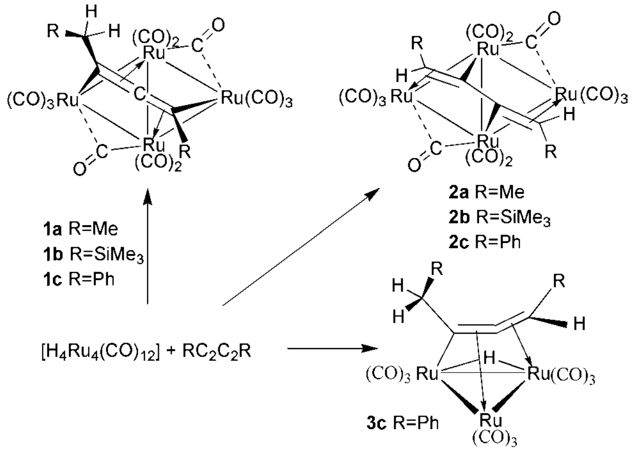

Scheme 2

Results and discussion

Reaction of $[Ru_4(\mu\text{-}H)_4(CO)_{12}]$ with MeC_2C_2Me

The thermolysis of a heptane solution of $[Ru_4(\mu\text{-}H)_4(CO)_{12}]$ and MeC_2C_2Me afforded two principal products in approximately equal yields, which were isolated on silica plates as dark red and maroon bands, generating highly soluble oily solids. Both compounds were formulated as $[Ru_4(CO)_{12}(Me_2C_4H_2)]$ **1a**, **2a** on the basis of their mass spectra and fully characterised spectroscopically (Table 1).

The ^1H NMR spectrum of compound **1a** shows a methylene quartet at δ 3.07, a methyl triplet at δ 1.47 and Me singlet at δ 2.87. This is consistent with the asymmetric 1,1-hydrogenation of the diyne ligand, accompanied by loss of a molecule of H_2, to produce $[Ru_4(CO)_{12}\{\mu_4\text{-}\eta^1:\eta^2:\eta^2:\eta^1\text{-}(MeCH_2C_3Me)\}]$ **1a** containing a novel 1,2-diene-1,3-diyl (allene-1,3-diyl) ligand, one carbon atom derived from the diyne becoming fully saturated. The IR spectrum exhibits an absorption at 1936 cm^{-1} which can be attributed to the semi-bridging CO interactions, while signals in the range 2092–2004 cm^{-1} are attributed to the presence of terminal carbonyls. The ^{13}C NMR spectrum shows two singlet resonances in a 1 : 2 ratio in the CO region at δ 198.43 and 189.00, indicating that two groups of ligands undergo independent fluxional processes on the NMR timescale at 25 °C.

The ^1H NMR spectrum of compound **2a** shows an allylic proton resonance as a single quartet at δ 4.25 and the methyl groups are also equivalent and observed as a doublet at δ 1.73, consistent with the molecules containing a twofold axis in solution. This suggests the presence of a hexa-2,4-diene-3,4-diyl ligand in $[Ru_4(CO)_{12}\{\mu_4\text{-}\eta^2:\eta^1:\eta^1:\eta^2\text{-}(RCHC)_2\}]$ **2a**, *i.e.* a structure analogous to that of $[Ru_4(CO)_{12}(\mu_4\text{-}C_8H_{10})]$.[14] The 1,4 hydrogenation is accompanied by expulsion of a molecule of H_2 from the cluster. The carbonyl region of the IR spectrum includes an absorption at 1944 cm^{-1}, characteristic of semi-bridging CO ligands, and again the ^{13}C NMR data show the two singlet resonances in the terminal carbonyl region at δ 198.12 and 189.00 in a 1 : 2 ratio, suggesting that the carbonyl ligands undergo similar fluxional processes in solution to those of **1a**.

Reaction of $[Ru_4(\mu\text{-}H)_4(CO)_{12}]$ with $Me_3SiC_2C_2SiMe_3$

The thermolysis of a heptane solution of $[Ru_4(\mu\text{-}H)_4(CO)_{12}]$ in the presence of a slight excess of $Me_3SiC_2C_2SiMe_3$ results in the production of a brown solution which yields a maroon and a purple band when the crude mixture is chromatographed on silica plates. Both products **1b** and **2b** were isolated in 30% yield and characterised spectroscopically (Table 1). From the mass spectrometric evidence, coupled with the appearance of signals in the ^1H NMR spectra corresponding to the presence of $SiMe_3$ groups (δ 0.15 and 0.07 for **1b** and δ 0.26 for **2b**), it is reasonable to propose that these products are the 1,4-bis(trimethylsilyl) analogues of **1a** and **2a**, *viz.* $[Ru_4(CO)_{12}\{\mu_4\text{-}\eta^1:\eta^2:\eta^2:\eta^1\text{-}(Me_3Si)CH_2C_3(SiMe_3)\}]$ **1b** and $[Ru_4(CO)_{12}\{\mu_4\text{-}\eta^2:\eta^1:\eta^1:\eta^2\text{-}[(Me_3Si)CHC]_2\}]$ **2b**. They are extremely soluble in hydrocarbon solvents and attempted crystallisation was unsuccessful.

Reaction of $[Ru_4(\mu\text{-}H)_4(CO)_{12}]$ with PhC_2C_2Ph

Unlike the two previous reactions, heating of $[Ru_4(\mu\text{-}H)_4(CO)_{12}]$ and PhC_2C_2Ph in heptane, under reflux, affords three principal products. The first orange product, isolated in 35% yield, has a mass spectrum exhibiting a parent peak at *m*/*z* 734 (calc. 762), and the structure was subsequently established by a single crystal X-ray analysis as $[Ru_3(\mu\text{-}H)(CO)_9(\mu_3\text{-}\eta^2:\eta^2:\eta^1\text{-}PhCH_2C_3HPh)]$ **3c**. No similar product was observed in the reactions with MeC_2C_2Me and $Me_3SiC_2C_2SiMe_3$. However, in this case, under the reaction conditions the $[Ru_4H_4(CO)_{12}]$ tetrahedron has lost an '$Ru(CO)_3$' vertex and three hydrogen atoms have been transferred to the ligand (two to one C atom), while one remains bound to the metal core. The IR spectrum (Table 1) shows peaks in the terminal carbonyl region only and is comparable with that of related allenyl compounds (which may, for example, be obtained by the reaction of $[Ru_3(CO)_{12}]$ with an alkyne RC_2CH_2R, one of the methylene protons being transferred to the cluster).[17] The ^1H NMR spectrum, in CD_2Cl_2, shows the presence of one hydride ligand at δ −20.02, the alkenylic proton at δ 4.12, and the two geminal protons as a singlet at δ 2.78.

For the second product, the spectroscopic data (Table 1) indicate that it is the phenyl analogue of compound **1A**. There are six phenyl CH signals in the ^{13}C NMR of **1c** and a strong CH_2 resonance at δ 50.7. The ^1H NMR spectrum shows the geminal CH_2 protons as two doublets at δ 4.40 and 4.15. The observation of two discrete chemical environments on the NMR timescale for these geminal protons contrasts that of the analogous methyl product **1a** which exhibits a room temperature ^1H NMR spectrum which suggests that these protons are chemically equivalent. This observation is consistent with a fluxional interchange between these protons in the case of **1a**.

Similarly, spectroscopic data for the third product were consistent with it being the phenyl analogue of **2a**, *i.e.* $[Ru_4(CO)_{12}\{\mu_4\text{-}\eta^2:\eta^1:\eta^1:\eta^2\text{-}(PhCHC)_2\}]$ **2c**. The IR spectrum (Table 1) contains an absorption at 1943 cm^{-1}, characteristic of

Table 1 Spectroscopic data for the new compounds **1a**–**3c**

Compound	$\tilde{\nu}$(CO)/cm^{-1}(CH$_2$Cl$_2$)	^{1}H NMR (δ, *J*/Hz)^a	^{13}C NMR (δ)	Mass Spectroscopy,^{b} *m*/*z*
1a	2092 (w), 2076 (sh), 2071 (vs), 2065 (sh), 2029 (vs, br), 2004 (sh), 1936 (m, br)	3.07 (q, 2H, *J* = 7.68, CH$_2$), 2.87 (s, 3H, CH$_3$), 1.47 (t, 3H, *J* = 7.65, CH$_3$)	198.43 (s, 4C, CO), 189.00 (s, 8C, CO), 111.11 (s, 1C, CH$_3$), 88.37 (s, 1C, C (enyl), 81.09 (s, 1C, C (enyl), 38.51 (s, 1C, CH$_2$), 31.46 (s, 1C, C (allene)), 18.51 (s, 1C, CH$_3$)	820 (821)
2a	2091 (w, sh), 2079 (sh), 2064 (vs), 2033 (s), 2022 (sh), 2004 (sh), 1944 (m, br)	4.25 (q, 2H, CH, *J* 5.85), 1.73 (d, 6H, CH$_3$, *J* = 5.85)	^{c} 198.12 (s, 4C, CO), 189.00 (s, 8C, CO), 54.56 (s, 2C, CH), 23.16 (s, 2C, CH$_3$)	820 (821)
1b	2091 (m), 2070 (s), 2054 (s), 2034 (vs), 2023 (sh), 1955 (m, br)	4.23 (d, 1H, *J* = 12.18, CH), 4.06 (d, 1H, *J* 12.24, CH), 0.15 (s, 9H, Si (CH$_3$)), 0.07 (s, 9H, Si (CH$_3$))		937 (938)
2b	2090 (w), 2078 (sh), 2066 (vs), 2027 (vs), 2012 (sh), 1944 (w, br)	4.58 (s, 2H, CH), 0.26 (s, 9H, Si (CH$_3$))		937 (938)
1c	2094 (w), 2071 (vs), 2066 (sh), 2037 (sh), 2030 (vs), 2000 (sh), 1947 (w, br)	7.32–6.56 (m, 10H, Ph), 4.40 (d, 1H, *J* = 14.70, CH$_2$), 4.15 (d, 1H, *J* = 14.68, CH$_2$)	^{c} 197.70 (s, 4C, CO), 189.01 (s, 8C, CO), 142.20 (s, 1C, C^{ipso}), 140.78 (s, 1C, C^{ipso}), 129.35 (s, 2C, Ph), 128.75 (s, 2C, Ph), 128.47 (s, 2C, Ph), 127.91 (s, 2C, Ph), 127.76 (s, 1C, Ph), 127.33 (s, 1C, Ph), 50.74 (s, 1C, CH$_2$)	917 (945)
2c	2093 (w), 2080 (w), 2067 (vs), 2037 (s), 2014 (m, br), 1943 (w, br)	7.25–6.45 (m, 10H, Ph), 5.06 (s, 2H, CH)	197.29 (s, C, CO), 189.01 (s, C, CO), 157.17 (s, 2C, C (enyl), 141.56 (s, 2C, C^{ipso}), 128.19 (s, 2C, Ph), 127.43 (s, 4C, Ph), 126.45 (s, 4C, Ph), 56.89 (s, 2C, CH)	945 (945)
3c	2094 (m), 2080 (sh), 2066 (vs), 2042 (vs), 2024 (s), 2000 (m), 1981 (sh)	^{d} 7.46–6.18 (m, 10H, Ph), 4.12 (s, 1H, CH), 2.78 (s, 2H, CH$_2$), −20.02 (s, 1H, RuHRu)	197.53 (s, 9C, CO), 152.95, 143.00 (2s, 2C, C), 141.76, 138.53, (2s, 2C, C^{ipso}), 130.39 (s, 2C, Ph), 129.99 (s, 2C, Ph), 129.82 (s, 2C, Ph), 129.64 (s, 2C, Ph) 128.36 (s, 1C, Ph), 125.01 (s, 1C, Ph), 58.40 (s, 1C, CH), 49.97 (s, 1C, CH$_2$)	734 (762)

^{a} CDCl$_3$ sample solution. ^{b} Calculated values in parentheses. ^{c} Poorly resolved or weak spectra preclude complete assignment. ^{d} CD$_2$Cl$_2$ sample solution.

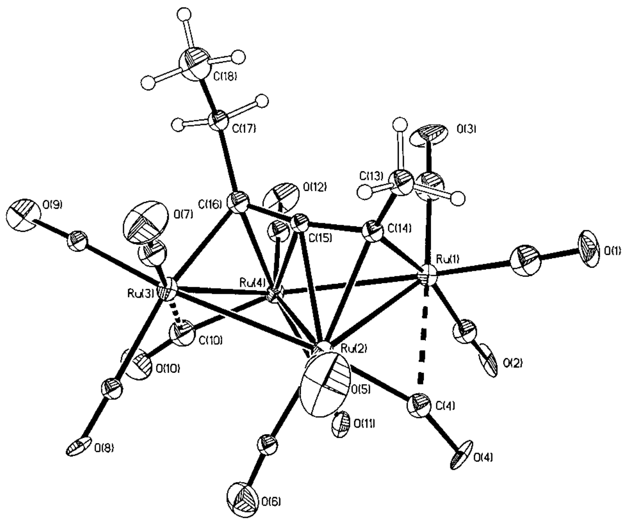

Fig. 1 Molecular structure of compound **1a** showing the atom numbering scheme; displacement ellipsoids are drawn at the 30% probability level (as in all Figures).

a semi-bridging CO ligand, along with signals corresponding to the presence of terminal carbonyls. The ^{13}C NMR spectrum shows two singlet resonances in the terminal carbonyl region at δ 197.29 and 189.01 in a 2:1 ratio as for **2a**. Three phenyl CH resonances are observed in the ^{13}C NMR as expected for two chemically equivalent, rotationally fluxional, phenyl groups. Similarly, three resonances are exhibited for the alkenic CH, *ipso* and enyl C atoms respectively in the ^{13}C NMR and the ^{1}H NMR spectrum exhibits a singlet at δ 5.06 characteristic of an allylic proton. These data are consistent with the molecule possessing average twofold symmetry in solution.

Table 2 Selected bond lengths (Å) and angles (°) for compound **1a**

Ru(1)–Ru(2)	2.763(3)	Ru(1)–C(4)	2.51(2)
Ru(2)–Ru(3)	2.898(2)	Ru(4)–C(16)	2.19(2)
Ru(1)–Ru(4)	2.900(2)	Ru(4)–C(15)	2.29(2)
Ru(3)–Ru(4)	2.768(3)	Ru(2)–C(15)	2.29(2)
Ru(2)–Ru(4)	2.717(3)	Ru(2)–C(14)	2.22(2)
Ru(1)–C(14)	2.07(2)	C(18)–C(17)	1.48(3)
Ru(3)–C(16)	2.07(2)	C(17)–C(16)	1.58(3)
Ru(3)–C(10)	2.52(2)	C(16)–C(15)	1.27(3)
Ru(4)–C(10)	1.91(2)	C(15)–C(14)	1.40(3)
Ru(2)–C(4)	1.96(2)	C(14)–C(13)	1.51(2)
Ru(1)–Ru(2)–Ru(3)	113.76(8)	Ru(2)–C(4)–O(4)	158(2)
Ru(1)–Ru(4)–Ru(3)	113.52(7)	Ru(4)–C(10)–O(10)	161(2)
Ru(2)–Ru(1)–Ru(4)	57.27(6)	Ru(2)–C(15)–Ru(4)	72.7(5)
Ru(1)–Ru(2)–Ru(4)	63.91(9)	C(13)–C(14)–C(15)	124(2)
Ru(1)–Ru(4)–Ru(2)	58.82(7)	C(14)–C(15)–C(16)	169(2)
Ru(2)–Ru(3)–Ru(4)	57.24(6)	C(15)–C(16)–C(17)	126(2)
Ru(3)–Ru(4)–Ru(2)	63.79(9)	C(16)–C(17)–C(18)	113(2)

Molecular structures of compounds 1a, 1c, 2a, 2c and 3c

The molecular and crystal structures of compounds **1a**, **1c**, **2a**, **2c** and **3c** have been determined by single-crystal X-ray diffraction and selected bond parameters are presented in Tables 2–6. The hexa-2,3-diene-2,4-diyl ligand in **1a** (Fig. 1) is bonded to all four metal atoms and donates a total of six electrons to the metal framework, giving a 62 electron count as expected for a butterfly geometry. To the best of our knowledge no structures exhibiting this coordination mode in tetranuclear complexes have been reported previously. C(16) and C(14) are σ-bound to the Ru(3) and Ru(1) wing-tip atoms respectively, both exhibiting typical Ru–C bond lengths of 2.07(2) Å. The two adjacent double bonds, C(14)–C(15) and C(15)–C(16), are aligned above the cluster hinge but in a diagonal fashion so

Table 3 Selected bond lengths (Å) and angles (°) for the two independent molecules of compound **1c**

Ru(1)–Ru(2)	2.779(4), 2.763(4)	Ru(1)–C(22)	2.58(3), 2.58(3)
Ru(2)–Ru(3)	2.916(3), 2.905(3)	Ru(4)–C(58)	2.22(3), 2.26(3)
Ru(1)–Ru(4)	2.902(3), 2.929(3)	Ru(4)–C(59)	2.23(3), 2.28(3)
Ru(3)–Ru(4)	2.763(4), 2.776(4)	Ru(2)–C(59)	2.24(3), 2.23(3)
Ru(2)–Ru(4)	2.753(4), 2.752(4)	Ru(2)–C(60)	2.26(3), 2.27(3)
Ru(1)–C(60)	2.12(3), 2.08(3)	C(57)–C(58)	1.56(4), 1.49(4)
Ru(3)–C(58)	2.09(3), 2.07(3)	C(58)–C(59)	1.32(4), 1.40(4)
Ru(3)–C(43)	2.54(4), 2.54(3)	C(59)–C(60)	1.37(4), 1.34(4)
Ru(4)–C(43)	1.87(4), 1.92(4)	C(60)–C(61)	1.52(4), 1.53(3)
Ru(2)–C(22)	1.91(3), 1.87(4)	C(51)–C(57)	1.54(3), 1.55(3)
Ru(1)–Ru(2)–Ru(3)	115.07(11), 116.00(11)	Ru(2)–C(22)–O(22)	162(3), 168(3)
Ru(1)–Ru(4)–Ru(3)	116.05(12), 114.86(11)	Ru(4)–C(43)–O(43)	160(4), 162(3)
Ru(2)–Ru(1)–Ru(4)	57.91(8), 57.75(8)	Ru(2)–C(59)–Ru(4)	76.0(10), 75.2(10)
Ru(1)–Ru(2)–Ru(4)	63.28(9), 64.14(9)	C(51)–C(57)–C(58)	113(2), 113(3)
Ru(1)–Ru(4)–Ru(2)	58.81(9), 58.11(9)	C(57)–C(58)–C(59)	125(3), 123(3)
Ru(2)–Ru(3)–Ru(4)	57.90(9), 57.90(9)	C(58)–C(59)–C(60)	162(3), 164(3)
Ru(3)–Ru(4)–Ru(2)	63.84(10), 63.42(10)	C(59)–C(60)–C(61)	125(3), 123(3)
Ru(3)–Ru(2)–Ru(4)	58.25(9), 58.68(9)		

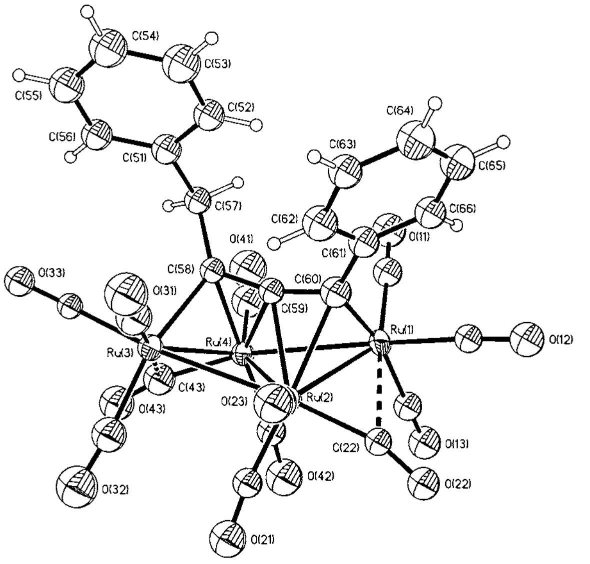

Fig. 2 Molecular structure of one of the two independent molecules of compound **1c**.

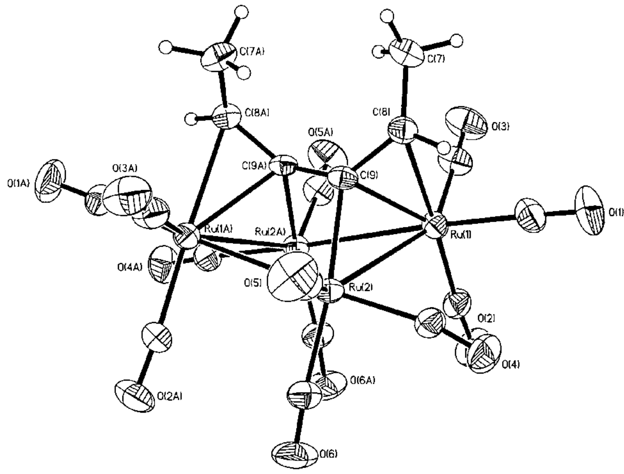

Fig. 3 Molecular structure of compound **2a**.

that only C(15) is positioned over the Ru(2)–Ru(4) vector, such that C(14)–C(15)–C(16) are approximately parallel to the Ru(1)–Ru(4) and Ru(2)–Ru(3) edges. The structure could thus be considered as two $M_3(\mu_3\text{-}\eta^2\text{-}\|)$ units fused *via* a M_2C face, in contrast to the cluster $[Ru_6(CO)_{14}(\mu\text{-SEt})_2(\mu_6\text{-}\eta^1:\eta^2:\eta^1:\eta^1:\eta^2:\eta^1\text{-MeC}_2C_2Me)]$[10] which might be regarded as two such units joined by a C–C and three Ru–Ru bonds in a butterfly arrangement. The two separate π interactions between C(15) and the two hinge atoms Ru(2) and Ru(4) (mean 2.29 Å) are considerably longer than the Ru–C σ distances, but only slightly longer than the C(14)–Ru(2) and C(16)–Ru(4) π distances (mean 2.21 Å).

Two of the carbonyl ligands, C(4)–O(4) and C(10)–O(10), deviate from linearity by 22(2) and 19(2)°, respectively, and appear to semi-bridge the ruthenium hinge–wing-tip edges, this interaction balancing the electronic requirements of the Ru(1) and Ru(3) vertices. The other ten carbonyl ligands are terminally bound and are approximately linear. The semi-bridged ruthenium edges of the butterfly are considerably shorter than the non-bridged edges [Ru(1)–Ru(2) 2.763(3), Ru(3)–Ru(4) 2.768(3), Ru(2)–Ru(3) 2.898(2), Ru(1)–Ru(4) 2.900(2) Å] while the hinge bond is shorter still [2.717(3) Å]. The dihedral angle between the two planes defined by the ruthenium atoms Ru(1)–Ru(2)–Ru(4) and Ru(2)–Ru(3)–Ru(4) is 144.9°, and does not lie in the narrow range (112–118°) commonly observed for pseudo-octahedral M_4C_2 systems. However, it has been shown by extended-Hückel calculations that whilst opening the angle is unfavourable for a cluster with 62 electrons, the potential energy is relatively soft and susceptible to the precise orientation of the ligands.[14]

The crystal structure of compound **1c** (Fig. 2), the phenyl analogue of **1a**, contains two chemically equivalent molecules in the asymmetric unit. The metal framework consists of a similar flattened butterfly core bridged by a 1,4-diphenylbuta-1,2-diene-1,3-diyl ligand, the geometry of the metal–carbon framework being very similar to that in **1a**; the Ru(2)–C(60), Ru(4)–C(58) and Ru(2)–C(59), Ru(4)–C(59) distances are not significantly different from the equivalent bonds in **1a**. The semi-bridging CO ligands C(22)–O(22) and C(43)–O(43) deviate from linearity by 18(3) [12(3)] and 20(3) [18(3)°] [the value in square brackets corresponds to that of the second independent molecule] whilst the other ten carbonyl ligands are terminally bound and essentially linear. The C(58)–C(59)–C(60) angle 162(3) [164(3)°] in the allenyl backbone is similar to that in the methyl analogue [169(2)°]. However, the dihedral angle between the two planes Ru(1)–Ru(2)–Ru(4) and Ru(3)–Ru(2)–Ru(4) is 150.2°, approximately 5° greater than that in **1a**. This is consistent with there being a twist of the C=C=C unit about the central carbon atom concomitant with the opening of the butterfly such that the π bonds to the central C atom and the π bonds remain the same length whilst the length of the σ bonds to the enyl C atoms increase in **1c** relative to **1a**.

The tetraruthenium skeleton of compound **2a** takes the form of a butterfly with crystallographic C_2 symmetry, bridged by a hexa-2,4-diene-3,4-diyl ligand (Fig. 3). The hexa-2,4-diene-

Table 4 Selected bond lengths (Å) and angles (°) for compound **2a**

Ru(1)–Ru(2)	2.7793(7)	Ru(2)–C(9)	2.068(5)
Ru(2)–Ru(2A)	2.8706(8)	C(7)–C(8)	1.500(8)
Ru(2)–Ru(2A)	2.8092(9)	C(8)–C(9)	1.394(7)
Ru(1)–C(8)	2.346(5)	C(9)–C(9A)	1.427(10)
Ru(1)–C(9)	2.266(5)		
Ru(1)–Ru(2)–Ru(2A)	61.82(2)	Ru(2)–C(9)–C(8)	130.4(4)
Ru(1)–Ru(2)–Ru(1A)	112.11(2)	Ru(2)–C(9)–C(9A)	101.3(2)
Ru(2)–Ru(1)–Ru(2A(	59.60(2)	C(7)–C(8)–C(9)	124.0(5)
Ru(2)–Ru(2A)–Ru(1)	58.58(2)	C(8)–C(9)–C(9A)	127.8(4)
Ru(1)–C(8)–C(9)	69.3(3)	Ru(2)–C(4)–O(4)	164.6(6)
Ru(1)–C(9)–C(9A)	110.4(4)		

Symmetry operator used to generate equivalent atoms: $-x, y, \frac{1}{2} - z$.

Table 5 Selected bond lengths (Å) and angles (°) for compound **2c**

Ru(1)–Ru(2)	2.7848(12)	Ru(3)–C(58)	2.335(8)
Ru(2)–Ru(3)	2.8865(10)	Ru(2)–C(59)	2.065(8)
Ru(1)–Ru(4)	2.8952(11)	Ru(4)–C(58)	2.083(9)
Ru(3)–Ru(4)	2.7662(13)	C(51)–C(57)	1.476(11)
Ru(2)–Ru(4)	2.8440(11)	C(57)–C(58)	1.391(11)
Ru(1)–C(60)	2.316(8)	C(58)–C(59)	1.441(11)
Ru(1)–C(59)	2.337(8)	C(59)–C(60)	1.414(11)
Ru(3)–C(57)	2.343(8)	C(60)–C(61)	1.478(12)
Ru(1)–Ru(2)–Ru(3)	115.39(3)	Ru(2)–C(59)–C(58)	100.8(5)
Ru(1)–Ru(4)–Ru(3)	115.71(3)	Ru(4)–C(58)–C(57)	131.4(6)
Ru(2)–Ru(1)–Ru(4)	60.05(3)	Ru(4)–C(58)–C(59)	96.9(6)
Ru(1)–Ru(2)–Ru(4)	61.90(3)	Ru(3)–C(22)–O(22)	167.0(9)
Ru(1)–Ru(4)–Ru(2)	58.05(3)	Ru(4)–C(43)–O(43)	169.8(11)
Ru(2)–Ru(3)–Ru(4)	60.37(3)	C(51)–C(57)–C(58)	127.7(8)
Ru(3)–Ru(4)–Ru(2)	61.91(3)	C(57)–C(58)–C(59)	130.0(8)
Ru(3)–Ru(2)–Ru(4)	57.72(3)	C(58)–C(59)–C(60)	129.0(7)
Ru(2)–C(59)–C(60)	129.2(6)	C(59)–C(60)–C(61)	126.7(7)

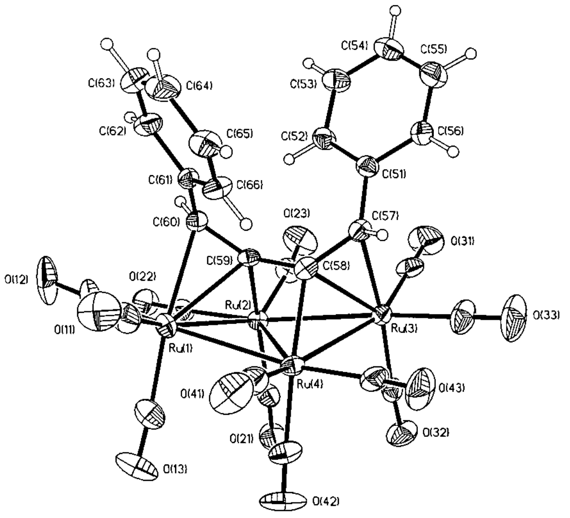

Fig. 4 Molecular structure of compound **2c**.

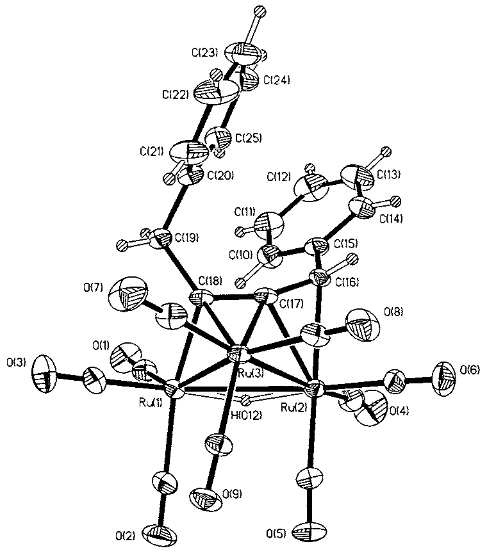

Fig. 5 Molecular structure of compound **3c**.

3,4-diyl ligand is bound to the cluster by four carbon atoms: C(9) and (9A) are σ-bound to the hinge atoms Ru(2) and Ru(2A) respectively, exhibiting typical bond lengths of 2.068(5) Å, the C(9)–C(9A) bond being aligned diagonally over the hinge vector. The ligand participates in two π interactions through C(7)/(7A) and C(8)/(8A) to the wing-tip vertices Ru(1)/(1A) with characteristically longer bonding interactions. The C–C bond lengths correspond to those typically observed for coordination allyl ligands. Two of the carbonyl ligands, C(4)–O(4) and C(4A)–O(4A), deviate from linearity by 15.6(6)° in a similar fashion to those in **1a** and appear to tend towards semi-bridging interactions with the wing-tip ruthenium atoms (the semi-bridged Ru–Ru edges are considerably shorter than the non-bridged edges as in **1a**). The dihedral angle between the two planes defined by the ruthenium atoms Ru(1)–Ru(2)–Ru(2A) and Ru(2A)–Ru(2)–Ru(1A) is 145.9°, only a small increase of 1° as compared to that of the allenediyl cluster **1a**.

The core framework of compound **2c** consists of a similar flattened butterfly structure bridged by a diphenylbuta-1,3-diene-2,3-diyl ligand (Fig. 4), although the molecule does not have exact C_2 symmetry and the conformations about the C–Ph rings differ slightly in the solid state. The dihedral angle between the two planes defined by the ruthenium atoms Ru(1)–Ru(2)–Ru(4) and Ru(3)–Ru(2)–Ru(4) is 155.8°, approximately 5° greater than that in **1c** and 10° greater than that in **1a** or **2a**. The dihedral angle in the previously reported analogue $[Ru_4(CO)_{12}(\mu_4\text{-}C_8H_{10})]$ is intermediate between these values at 150°.[14] The C–C and Ru–C bond lengths in these three examples are broadly similar, the main differences being in the π-bond lengths between the enyl carbon atoms and the hinge, which increase with increasing dihedral angle such that they are *ca.* 0.08 Å longer than the Ru–C(H) π distances in **2a** but strictly comparable in **2c**. In contrast, the dienediyl ligand is less strongly bound to the square face in $[Ru_4(CO)_{10}(\mu\text{-}CO)(\mu_4\text{-}PPh)(PhC(H)C_2C(H)Ph)]$,[13] with mean Ru–C σ bond lengths of 2.13, Ru–C(enyl) π 2.30 and Ru–C(H) π 2.47 Å, the difference in π bond lengths being significantly greater than that in **2a** or **2c** with a butterfly core geometry. The RC(H)=C–C angles in the cyclooctadienediyl compound [mean 123°] are significantly smaller than those in **2a** [127.8(4)] and **2c** [130.0(8), 129.0(7)] which is probably an artefact of strain in the C_8 ring.

The structure of compound **3c** is similar to that of the allenyl clusters reported previously[17] and consists of a closed ruthenium triangle with all three metal atoms coordinated to three terminal carbonyl ligands are bridged by the 1,4-diphenylbuta-1,2-dien-3-yl ligand (Fig. 5). The C(18) atom is σ-bound to Ru(1), C(18) and C(17) participate in a π interaction to Ru(3), while C(17) and C(16) are π-bound to Ru(2). The hydride was not directly located but potential energy calculations indicate that it bridges the Ru(1)–Ru(2) edge,[18] The C(4)–O(4) and C(11)–O(11) ligands being splayed out from the coordination site of the hydride atom. The C(18)–Ru(1) bond length is 2.068(4) Å, characteristic of a Ru–C σ bond. The Ru(3)–C(17) and Ru(3)–C(18) bond lengths are 2.124(4) and 2.260(4) Å, respectively, while the Ru(2)–C(16) bond distance is 2.363(4) and Ru(2)–C(17) is 2.263(4) Å. The C(18)–C(17) and the C(17)–C(16) bond distances are similar and characteristic of adjacent alkenylic C–C distances. The allenylic angle C(16)–C(17)–C(18) of 143.7(4)° is consistent with that in similar ligands, *e.g.* 143.0° in $[Ru_3(\mu\text{-}H)(CO)_9(\mu_3\text{-}\eta^1:\eta^2:\eta^2\text{-}$

Table 6 Selected bond lengths (Å) and angles (°) for compound **3c**

Ru(1)–Ru(2)	2.9988(8)	Ru(2)–C(16)	2.363(4)
Ru(2)–Ru(3)	2.7930(9)	C(17)–C(18)	1.365(7)
Ru(1)–Ru(3)	2.7531(9)	C(16)–C(17)	1.393(9)
Ru(1)–C(18)	2.068(4)	C(18)–C(19)	1.524(6)
Ru(3)–C(18)	2.260(4)	C(19)–C(20)	1.527(7)
Ru(3)–C(17)	2.124(4)	C(16)–C(15)	1.502(6)
Ru(2)–C(17)	2.263(4)		
Ru(1)–Ru(2)–Ru(3)	56.63(2)	C(15)–C(16)–C(17)	122.8(4)
Ru(1)–Ru(3)–Ru(2)	65.46(2)	C(16)–C(17)–C(18)	143.7(4)
Ru(2)–Ru(1)–Ru(3)	57.91(2)	C(17)–C(18)–C(19)	123.4(4)
Ru(1)–C(18)–C(17)	109.3(3)	C(18)–C(19)–C(20)	116.2(4)
Ru(2)–C(17)–C(18)	114.7(3)		

$C_8H_{11})]$,[19] but much smaller than that in the allenediyl clusters **1a**,**1c**.

It is interesting that no clusters were isolated in which a 1,2 hydrogenation had occurred to generate a eneyne ligand. It was not possible to isolate a 60 electron butterfly cluster of the form $[Ru_4(CO)_{12}(\mu_4\text{-}\eta^2\text{-}RCCC(H)C(H)R)]$, analogous to $[Ru_4(CO)_{12}(\mu_4\text{-}\eta^2\text{-}C_8H_{10})]$ which was obtained as the 1,2-dehydrogenation product in the thermolysis of 1,3-cyclooctadiene with $[Ru_3(CO)_{12}]$.[14] In contrast, the 60 electron butterfly cluster $[Ru_4(CO)_{12}(\mu_4\text{-}\eta^2\text{-}PhC_2C_2Ph)]$, in which one of the alkyne functions remains uncoordinated, is isolated as one of the products in the reaction of PhC_2C_2Ph with $[Ru_3(CO)_{10}(NCMe)_2]$.[4] It is also notable that the thermolysis of C_8H_{12} with $[Ru_3(CO)_{12}]$ did not yield a cluster analogous to **1** that displays the allenediyl bonding mode, perhaps because an angle of *ca.* 162° in the allene unit would induce too much strain in the C_8 ring, although an angle of 143° is observed in the allenyl compound $[Ru_3(\mu\text{-}H)(CO)_9(\mu_3\text{-}\eta^1:\eta^2:\eta^2\text{-}C_8H_{11})]$.

Conclusion

The reaction of diynes with $[Ru_4H_4(CO)_{12}]$ leads to 1,1 or 1,4-dihydrogenation of the diyne to generate novel allene-1,3-diyl or a 1,3-diene-2,3-diyl ligands respectively (with cleavage of one Ru–Ru edge and loss of H_2) which bond to all four Ru atoms of a butterfly cluster. This differs from the behaviour of the cluster $[Ru_4(CO)_{12}(\mu_4\text{-}PPh)]$ studied previously, in which 1,2 or 1,4 dihydrogenation was the predominant reaction pathway. In addition, Ru–Ru bond cleavage may occur with transfer of an additional H atom to the ligand, thus generating an allenyl ligand in the familiar $\mu_3\text{-}\eta^1:\eta^2:\eta^2$ bonding mode.

Experimental

Reactions and general manipulations were carried out using standard Schlenk apparatus under an atmosphere of dry, oxygen-free N_2 and solutions were stirred magnetically unless otherwise stated. All solvents were degassed and dried by distillation over an appropriate drying agent. CH_2Cl_2 solution IR spectra in the carbonyl region (2200–1700 cm^{-1}) were recorded on a Perkin-Elmer 1710 spectrometer using NaCl cells of 0.5 mm path lengths. Reactions were monitored routinely by IR spectrometry. Low resolution FAB mass spectra were recorded on a AE1/Kratos MS 50 spectrometer, ^1H and ^{13}C NMR spectra on a Bruker AM 400 FT spectrometer in appropriate deuteriated solvents. Chemical shifts were referenced to residual protons in $CDCl_3$ (δ 7.25) for ^1H and to $CDCl_3$ (δ 77.0) for ^{13}C. The products were separated either by column chromatography on silica gel (230–400 mesh) or on glass plates (20 × 20 cm) coated with *ca.* 2 mm of silica gel (type 60 GF254 Merck) prepared in this laboratory. Hexa-2,4-diyne, 1,4-bis(trimethylsilyl) butadiyne and 1,4-diphenylbutadiyne were used as obtained commercially without further purification. $[Ru_4H_4(CO)_{12}]$ was prepared by the literature procedure.[20]

Reactions of $[Ru_4H_4(CO)_{12}]$

With MeC_2C_2Me. $[Ru_4H_4(CO)_{12}]$ (150 mg, 0.21 mmol) was dissolved and stirred in heptane (20 cm^3), MeC_2C_2Me (18.5 mg, 0.24 mmol) added and the mixture heated under reflux for 3 h. The resulting brown heptane solution was evaporated to dryness under reduced pressure. The crude products were separated on silica plates using hexane as eluent, affording $[Ru_4(CO)_{12}\{\mu_4\text{-}\eta^1:\eta^2:\eta^2:\eta^1\text{-}(MeCH_2C_3Me)\}]$ **1a** (high R_f) as a maroon air-stable solid (45%) and $[Ru_4(CO)_{12}\{\mu_4\text{-}\eta^2:\eta^1:\eta^1:\eta^2\text{-}(MeCHC_2CHMe)\}]$ **2a** (45%) (low R_f) as a purple, air-unstable solid. **1a** and **2a** were recrystallised from a CH_2Cl_2–pentane solution at −30 °C, affording dark red air-stable blocks and purple blocks respectively. **1a**, found: C, 39.98; H, 1.25%. Calc. for $C_9H_4O_6Ru_2$: C, 40.92; H, 1.21%. **2a**, found, C, 41.23; H, 1.30%. Calc. for $C_9H_4O_6Ru_2$: C, 40.92; H, 1.21%.

With $Me_3SiC_2C_2SiMe_3$. $[Ru_4H_4(CO)_{12}]$ (150 mg, 0.21 mmol) was dissolved and stirred in heptane (20 cm^3), $Me_3SiC_2C_2SiMe_3$ (48 mg, 0.24 mmol) added and the mixture heated under reflux for 3 h. The resultant brown heptane solution was evaporated to dryness under high vacuum. The crude oily residue was separated on silica TLC plates using pentane as eluent, affording $[Ru_4(CO)_{12}\{\mu_4\text{-}\eta^1:\eta^2:\eta^2:\eta^1\text{-}(Me_3Si)CH_2C_3(SiMe_3)\}]$ **1b** as a maroon, air-stable oily solid (30%) and $[Ru_4(CO)_{12}\{\mu_4\text{-}\eta^2:\eta^1:\eta^1:\eta^2\text{-}(Me_3Si)CHC_2CH(SiMe_3)\}]$ **2b** (30%) (low R_f) as a purple, air-stable oily solid.

With PhC_2C_2Ph. $[Ru_4H_4(CO)_{12}]$ (150 mg, 0.21 mmol) was dissolved in heptane (20 cm^3), 1,4-diphenylbuta-1,3-diyne (50 mg, 0.24 mmol) added and the mixture heated under reflux for 3 h. The resulting brown heptane solution was evaporated to dryness under reduced pressure. The crude residue was separated on silica TLC plates using hexane as eluent. This afforded $[Ru_3H(CO)_9\{\mu_3\text{-}\eta^2:\eta^2:\eta^1\text{-}(PhCH_2C_3HPh)\}]$ **3c** (high R_f) as an orange air-stable solid (35%), $[Ru_4(CO)_{12}\{\mu_4\text{-}\eta^1:\eta^2:\eta^2;\eta^1\text{-}(PhCH_2C_3Ph)\}]$ **1c** as a maroon, air-stable oily solid (25%) and $[Ru_4(CO)_{12}\{\mu_4\text{-}\eta^2:\eta^1:\eta^1:\eta^2\text{-}(PhCHC_2CHPh)\}]$ **2c** (30%) (low R_f) as a purple, air-unstable oily solid. **1c**, **2c** and **3c** were recrystallised from a CH_2Cl_2–pentane solution at −30 °C, affording black plates, dark purple blocks and orange air-stable blocks respectively. **1c**, found: C, 35.41; H, 1.20%. Calc. for $C_7H_3O_3Ru$: C, 35.59; H, 1.27%. **2c**, found: C, 35.16; H, 1.35%. Calc. for $C_7H_3O_3$ Ru: C, 35.59; H, 1.27%. **3c**, found: C, 39.31; H, 1.68%. Calc. for $C_{25}H_{14}O_9Ru_3$: C, 39.16; H, 1.83%.

Crystal structure determination of compounds 1a, 1c, 2a, 2c and 3c

Data were collected by the ω–2θ (**2a**, **2c**, **3c**) or ω (**1a**, **1c**) scan method on a Rigaku AFC5R (**1c**, **2c**, **3c**) and a AFC7R (**1a**, **2a**) four circle diffractometer. Three standard reflections measured at intervals of 200 showed no significant variation in intensity. Cell parameters were obtained by least-squares refinement on diffractometer angles from 25 centred reflections ($12.5 < 2\theta < 20°$). Semi-empirical absorption corrections based on ψ-scan data were applied.[21] The structures were solved by direct methods (heavy atom positions) and subsequent Fourier differences syntheses (SHELXTL PLUS[22]) and refined anisotropically on all non-H atoms (**2a**, **2c**, **3c**), Ru and O (**1a**) or Ru atoms alone (**1c**) by full-matrix least-squares on F^2 (SHELXL 97[23]). Hydrogen atoms were placed in geometrically idealised positions and refined using a riding model or as rigid methyl groups. In the final cycles of refinement a weighting scheme was introduced which produced a flat analysis of variance. Crystal data and refinement details are summarised in Table 7.

CCDC reference number 186/2236.

See http://www.rsc.org/suppdata/dt/b0/b006810l/ for crystallographic files in .cif format.

Table 7 Crystal data and refinement details for compounds **1a**,**1c**, **2a**,**2c** and **3c**[a]

	1a	**2a**	**1c**	**2c**	**3c**
Molecular formula	$C_{18}H_8O_{12}Ru_4$	$C_{18}H_8O_{12}Ru_4$	$C_{28}H_{12}O_{12}Ru_4$	$C_{28}H_{12}O_{12}Ru_4$	$C_{25}H_{14}O_9Ru_3$
M	820.52	820.52	944.66	944.66	761.57
Crystal system	Orthorhombic	Monoclinic	Orthorhombic	Monoclinic	Triclinic
Space group	$P2_12_12_1$	$C2/c$	$Pna2_1$	$P2_1/n$	$P\bar{1}$
a/Å	11.020(4)	13.257(3)	19.012(4)	10.748(3)	10.457(3)
b/Å	21.034(7)	9.861(2)	9.359(2)	18.891(4)	13.594(5)
c/Å	10.018(12)	19.176(3)	34.315(7)	15.778(3)	9.919(2)
α/°					100.90(2)
β/°		111.640(10)		107.870(1)	105.55(2)
γ/°					78.18(3)
U/Å^3	2322(3)	2330.1(8)	6106(2)	3049.0(12)	1316.1(7)
Z	4	4	8	4	2
μ/mm^{-1}	2.612	2.603	2.002	2.005	1.749
T/K	153(2)	293(2)	293(2)	293(2)	293(2)
Reflections measured	4093	2788	4062	5672	6375
Independent reflections	3050 (R_{int} = 0.118)	2675 (R_{int} = 0.031)	4062 (R_{int} = 0.00)	5370 (R_{int} = 0.038)	6039 (R_{int} = 0.029)
Parameters, restraints	217, 0	155, 0	345, 0	397, 0	334, 0
$wR2$ (all data)	0.1285	0.1709	0.1768	0.2145	0.1443
$R1[I > 2\sigma(I)]$	0.0631	0.0356	0.0602	0.0443	0.0441
Observed reflections	2189	2141	2877	3298	5196
Absolute structure parameter	0.1(2)		0.1(15)		

[a] Data in common: graphite-monochromated Mo-Kα radiation, $\lambda = 0.71073$ Å.

Acknowledgements

We gratefully acknowledge the financial support of the EPSRC (L. P. C., G. P. S.) and the Cambridge Crystallographic Data Centre (J. E. D., G. P. S.). We also thank the European Union for INTAS grant no. 97-3199 that has supported this research.

References

1 E. Sappa, A Tiripicchio and P. Braunstein, *Chem. Rev.*, 1983, **83**, 203; P. R. Raithby and M. J. Rosales, *Adv. Inorg. Radiochem.*, 1985, **29**, 169.
2 M. I. Bruce, P. J. Low, A. Werth, B. W. Skelton and A. H. White, *J. Chem. Soc.*, *Dalton Trans.*, 1996, 1551.
3 B. F. G. Johnson, J. Lewis, C. E. Housecroft, M. A. Gallop, M. Martinelli, D. Braga and F. Grepioni, *J. Mol. Catal.*, 1992, **74**, 61; B. F. G. Johnson, *J. Organomet. Chem.*, 1994, **475**, 31.
4 M. I. Bruce, B. W. Skelton, A. H. White and N. N. Zaitseva, *J. Chem. Soc.*, *Dalton Trans.*, 1996, 3151; M. I. Bruce, B. W. Skelton, A. H. White and N. N. Zaitseva, *Inorg. Chem. Commun.*, 1998, **1**, 134; M. I. Bruce, B. W. Skelton, A. H. White and N. N. Zaitseva, *J. Organomet. Chem.*, 1998, **558**, 197.
5 C. S.-W. Lau and W.-T. Wong, *J. Chem. Soc.*, *Dalton Trans.*, 1999, 2511.
6 M. G. Karpov, S. P. Tunik, V. R. Denisov, G. L. Starova, A. B. Nikolskii, F. M. Dolgushin, A. I. Yanovsky and Yu. T. Struchkov, *J. Organomet. Chem.*, 1995, **485**, 219; S. P. Tunik, E. V. Grachova, V. R. Denisov, G. L. Starova, A. B. Nikolskii, F. M. Dolgushin, A. I. Yanovsky and Yu. T. Struchkov, *J. Organomet. Chem.*, 1996, **536**, 339.
7 M. I. Bruce, N. N. Zaitseva, B. W. Skelton and A. H. White, *J. Organomet. Chem.*, 1997, **536–537**, 93.
8 J. F. Corrigan, S. Doherty, N. J. Taylor and A. J. Carty, *Organometallics*, 1993, **12**, 1365; J. F. Corrigan, S. Doherty, N. J. Taylor and A. J. Carty, *Organometallics*, 1992, **11**, 3167.
9 Y. Chi, A. J. Carty, P. Blenkiron, E. Delgado, G. D. Enright, W. Wang, S.-M. Peng and G.-H. Lee, *Organometallics*, 1996, **15**, 5269; M. I. Bruce, B. W. Skelton, A. H. White and N. N. Zaitseva, *J. Chem. Soc.*, *Dalton Trans.*, 1999, 13.
10 S. Jeannin, Y. Jeannin, F. Robert and C. Rosenberger, *Inorg. Chem.*, 1994, **33**, 243.
11 B. J. Bobbie, N. J. Taylor and A. J. Carty, *J. Chem. Soc.*, *Chem. Commun.*, 1991, 1511.
12 C. J. Adams, M. I. Bruce, B. W. Skelton and A. H. White, *J. Chem. Soc.*, *Dalton Trans.*, 1999, 1283; 2451; C. J. Adams, M. I. Bruce, B. W. Skelton and A. H. White, *J. Organomet. Chem.*, 1999, **584**, 254.
13 J. F. Corrigan, N. J. Taylor and A. J. Carty, *Organometallics*, 1994, **13**, 3778.
14 D. Braga, F. Grepioni, D. B. Brown, B. F. G. Johnson and M. J. Calhorda, *Organometallics*, 1996, **15**, 5721.
15 L. P. Clarke, J. E. Davies, P. R. Raithby and G. P. Shields, *J. Chem. Soc.*, *Dalton Trans.*, 1996, 4147.
16 E. Sappa, A. M. M. Lanfredi, G. Predieri and A. Tiripiccio, *Inorg. Chim. Acta*, 1982, **61**, 217; S. Aime, G. Gervasio, L. Milone, E. Sappa and M. Franchini-Angela, *Inorg. Chim. Acta*, 1978, **27**, 145; G. Gervasio, E. Sappa, A. M. Mannotti Lanfredi and A. Tiripicchio, *Inorg. Chim. Acta*, 1983, **68**, 171.
17 See, for example, G. Gervasio, D. Osella and M. Valle, *Inorg. Chem.*, 1976, **15**, 1221; C. E. Shuchart, G. H. Young, A. Wojcicki, M. Calligaris and G. Nardin, *Organometallics*, 1990, **9**, 2417; C. E. Shuchart, A. Wojcicki, M. Calligaris, P. Faleschini and G. Nardin, *Organometallics*, 1994, **13**, 1999; D. Nucciarone, N. J. Taylor and A. J. Carty, *Organometallics*, 1984, **3**, 177; D. Nucciarone, S. A. MacLaughlin, N. J. Taylor and A. J. Carty, *Organometallics*, 1988, **7**, 106; J. Saudes, F. Dahan and R. Mathieu, *Organometallics*, 1988, **7**, 47.
18 A. G. Orpen, *J. Chem. Soc.*, *Dalton Trans.*, 1980, 2509.
19 D. Braga, F. Grepioni, D. B. Brown, B. F. G. Johnson and M. J. Calhorda, *J. Organomet. Chem.*, 1996, **513**, 1996.
20 B. F. G. Johnson, R. D. Johnston, J. Lewis and B. H. Robinson, *Chem. Commun.*, 1966, 851; J. W. S. Jamieson, J. V. Kingston and G. Wilkinson, *Chem. Commun.*, 1966, 5669; S. A. R. Knox, J. W. Koepke, M. A. Andrews and H. D. Kaesz, *J. Am. Chem. Soc.*, 1975, **97**, 3942.
21 TEXSAN, Version 1.7-1, Molecular Structure Corporation, The Woodlands, TX, 1985, 1992, 1995; A. C. T. North, D. C. Phillips and F. S. Mathews, *Acta Crystallogr.*, *Sect. A*, 1968, **24**, 351.
22 SHELXTL PLUS, PC Release 4.1, Siemens Analytical X-Ray Instruments Inc., Madison, WI, 1991.
23 G. M. Sheldrick, SHELXL 97, University of Göttingen, 1997.